Bioorganic Chemistry 92 (2019) 103276

Contents lists available at ScienceDirect

Bioorganic Chemistry

journal homepage: www.elsevier.com/locate/bioorg

Antiprotozoal activities of marine polyether triterpenoids

Ana R. Díaz-Marrero[a,1], Atteneri López-Arencibia[b,1], Carlos J. Bethencout-Estrella[b], Francisco Cen-Pacheco[a,c], Ines Sifaoui[b], Alberto Hernández Creus[d], María Clara Duque-Ramírez[b], María L. Souto[a,e], Antonio Hernández Daranas[a,f], Jacob Lorenzo-Morales[b], José E. Piñero[b,*], José J. Fernández[a,e,*]

[a] Instituto Universitario de Bio-Orgánica Antonio González (IUBO AG), Centro de Investigaciones Biomédicas de Canarias (CIBICAN), Universidad de La Laguna (ULL), Avda. Astrofísico F. Sánchez 2, 38206 La Laguna, Tenerife, Spain
[b] Instituto Universitario de Enfermedades Tropicales y Salud Pública de Canarias (IETSPC), Universidad de La Laguna (ULL), Avda. Astrofísico F. Sánchez s/n, 38206 La Laguna, Tenerife, Spain
[c] Facultad de Bioanálisis, Campus-Veracruz, Universidad Veracruzana (UV), Veracruz 91700, Mexico
[d] Departamento de Química, Área de Química Física, Instituto de Materiales y Nanotecnología, Universidad de La Laguna (ULL), Avda. Astrofísico F. Sánchez s/n, 38206 Tenerife, Spain
[e] Departamento de Química Orgánica, Universidad de La Laguna (ULL), Avda. Astrofísico F. Sánchez 2, 38206 La Laguna, Tenerife, Spain
[f] Instituto de Productos Naturales y Agrobiología (IPNA), Consejo Superior de Investigaciones Científicas (CSIC), Avda. Astrofísico F. Sánchez s/n, 38206 Tenerife, Spain

ARTICLE INFO

Keywords:
Marine natural products
Marine polyether
Oxasqualenoids
Kinetoplastids
Laurencia
Leishmania
Leishmanicidal
Trypanosoma
Trypanocidal

ABSTRACT

Chagas disease and leishmaniasis are tropical neglected diseases caused by kinetoplastids protozoan parasites of *Trypanosoma* and *Leishmania* genera, and a public health burden with high morbidity and mortality rates in developing countries. Among difficulties with their epidemiological control, a major problem is their limited and toxic treatments to attend the affected populations; therefore, new therapies are needed in order to find new active molecules. In this work, sixteen *Laurencia* oxasqualenoid metabolites, natural compounds **1–11** and semisynthetic derivatives **12–16**, were tested against *Leishmania amazonensis*, *Leishmania donovani* and *Trypanosoma cruzi*. The results obtained point out that eight substances possess potent activities, with IC_{50} values in the range of 5.40–46.45 μM. The antikinetoplastid action mode of the main metabolite dehydrothyrsiferol (**1**) was developed, also supported by AFM images.

The semi-synthetic active compound 28-iodosaiyacenol B (**15**) showed an IC_{50} 5.40 μM against *Leishmania amazonensis*, turned to be non-toxic against the murine macrophage cell line J774A.1 (CC_{50} > 100). These values are comparable with the reference compound miltefosine IC_{50} 6.48 ± 0.24 and CC_{50} 72.19 ± 3.06 μM, suggesting that this substance could be scaffold for development of new antikinetoplastid drugs.

1. Introduction

Protozoal diseases, such as leishmaniasis and American trypanosomiasis (Chagas disease) are the cause of considerable morbidity throughout the world, affecting millions every year [1]. Leishmaniasis is a disease caused by parasites of the genus *Leishmania* and is transmitted by the bite of a female phlebotomine sand fly. Leishmaniasis can manifest in three different forms: cutaneous and mucocutaneous, caused by *Leishmania amazonensis*, and visceral, originated by infections with *L. donovani* [2]. Chagas disease affects around 8 million people worldwide and the available treatment is just effective in the acute phase of the illness. Current therapy against these diseases involves the use of benznidazole or nifurtimox (Chagas) and amphotericin B (*Leishmania*), which present toxic side effects and the risk of resistant-strains emergence [3].

Interestingly till date, those diseases have remained significant, despite our advances in antimicrobial chemotherapy and supportive care, mostly due to problems associated with chemotherapeutic interventions. In fact, the treatment of these infections has been undermined by resistance, variable efficacy between strains or species, toxicity, parenteral administration, requirement for long courses of administration and adverse effects and cost. In recent years, studies on natural compounds have taken relevance, and among them marine organisms are being evaluated for the search of new potential antiparasitic agents.

* Corresponding authors.
E-mail addresses: jpinero@ull.edu.es (J.E. Piñero), jjfercas@ull.edu.es (J.J. Fernández).
[1] These authors contributed equally to this manuscript.

https://doi.org/10.1016/j.bioorg.2019.103276
Received 24 July 2019; Received in revised form 4 September 2019; Accepted 11 September 2019
Available online 11 September 2019

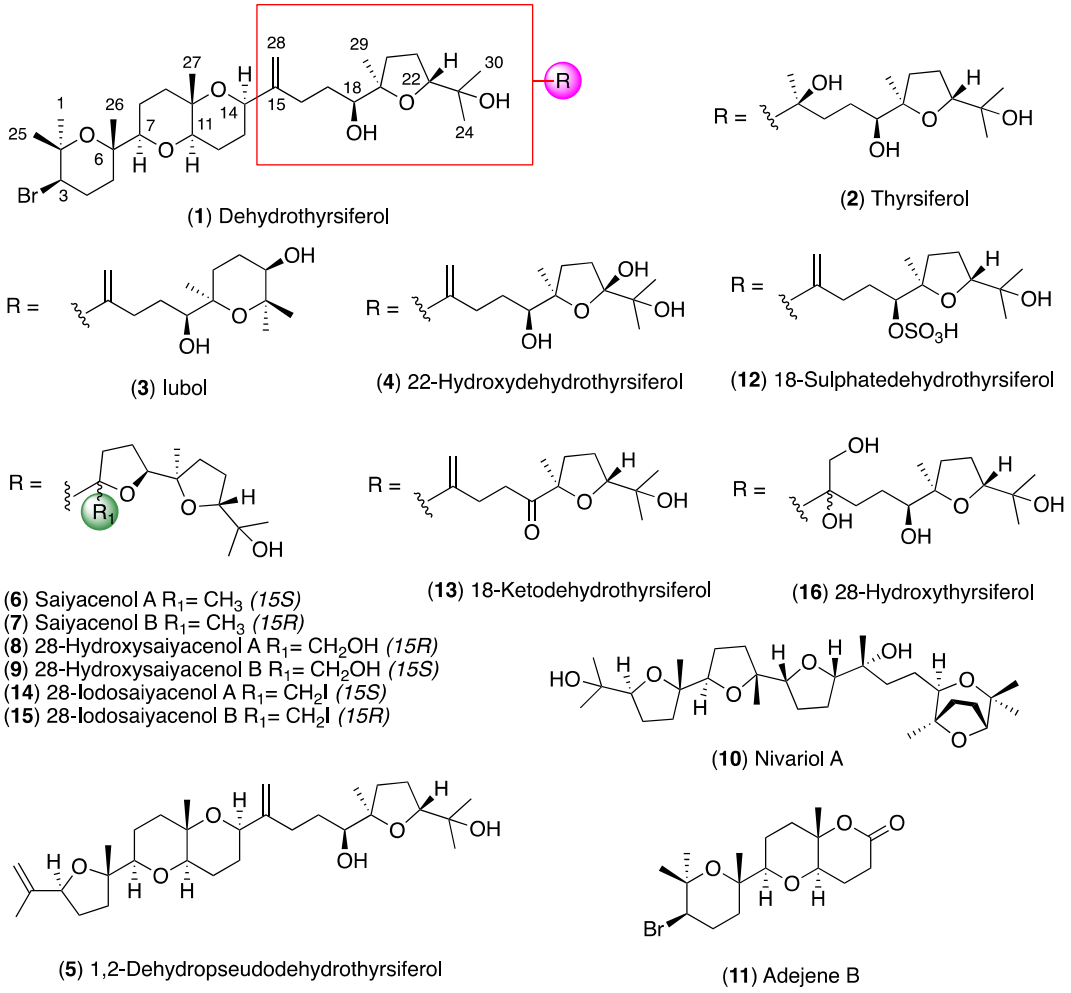

Fig. 1. Structure of the natural (**1**-**11**) and semi-synthetic (**12**-**16**) tested terpenoid polyether compounds.

Within this marine chemical arsenal, molecules with exciting biological activities include polyether compounds, such as the squalene-derived metabolites isolated from the red alga *Laurencia*. In fact, a large number of triterpene polyether compounds with significant structural and pharmacological diversity have been identified. Within this family, compounds with moderate to potent cytotoxic activity have been

Table 1
Anti-kinetoplastid effect of natural and semi-synthetic oxasqualenoids **1**-**16** against *Leishmania amazonensis, Leishmania donovani* and *Trypanosoma cruzi*. IC_{50} are reported in μM. Toxicity against murine macrophage J774.A1 (CC_{50}).

Compounds	*L. amazonensis* (Promastigote)	*L. donovani* (Promastigote)	*T. cruzi* (Epimastigote)	Murine macrophage J774A.1
1	8.36 ± 0.77	28.26 ± 1.74	9.45 ± 0.46	28.77 ± 3.10
2	NA	NA	NA	> 100
3	7.00 ± 0.22	18.08 ± 2.62	9.20 ± 1.16	7.72 ± 0.22
4	34.65 ± 0.22	NA	NA	> 100
5	NA	NA	NA	> 100
6	12.96 ± 1.84	NA	13.75 ± 2.28	59.91 ± 8.50
7	10.32 ± 1.09	NA	NA	> 100
8	NA	NA	NA	> 100
9	NA	NA	NA	> 100
10	NA	NA	NA	> 100
11	NA	NA	NA	> 100
12	NA	NA	NA	> 50
13	38.53 ± 9.28	46.45 ± 2.26	11.02 ± 2.60	23.37 ± 1.76
14	20.39 ± 2.90	33.90 ± 1.74	NA	29.45 ± 0.20
15	5.40 ± 0.13	16.18 ± 0.22	NA	> 100
16[1]	NA	NA	NA	> 100
Miltefosine *	6.48 ± 0.24	3.32 ± 0.27		72.19 ± 3.06
Benznidazole*			6.94 ± 1.94	400 ± 4.00

NA: Not active at the maximum concentration tested 200 μM against parasites.
* Reference compounds.
[1] These values correspond to a synthetic sample that contain a mixture of *16R and 16S stereoisomers*.

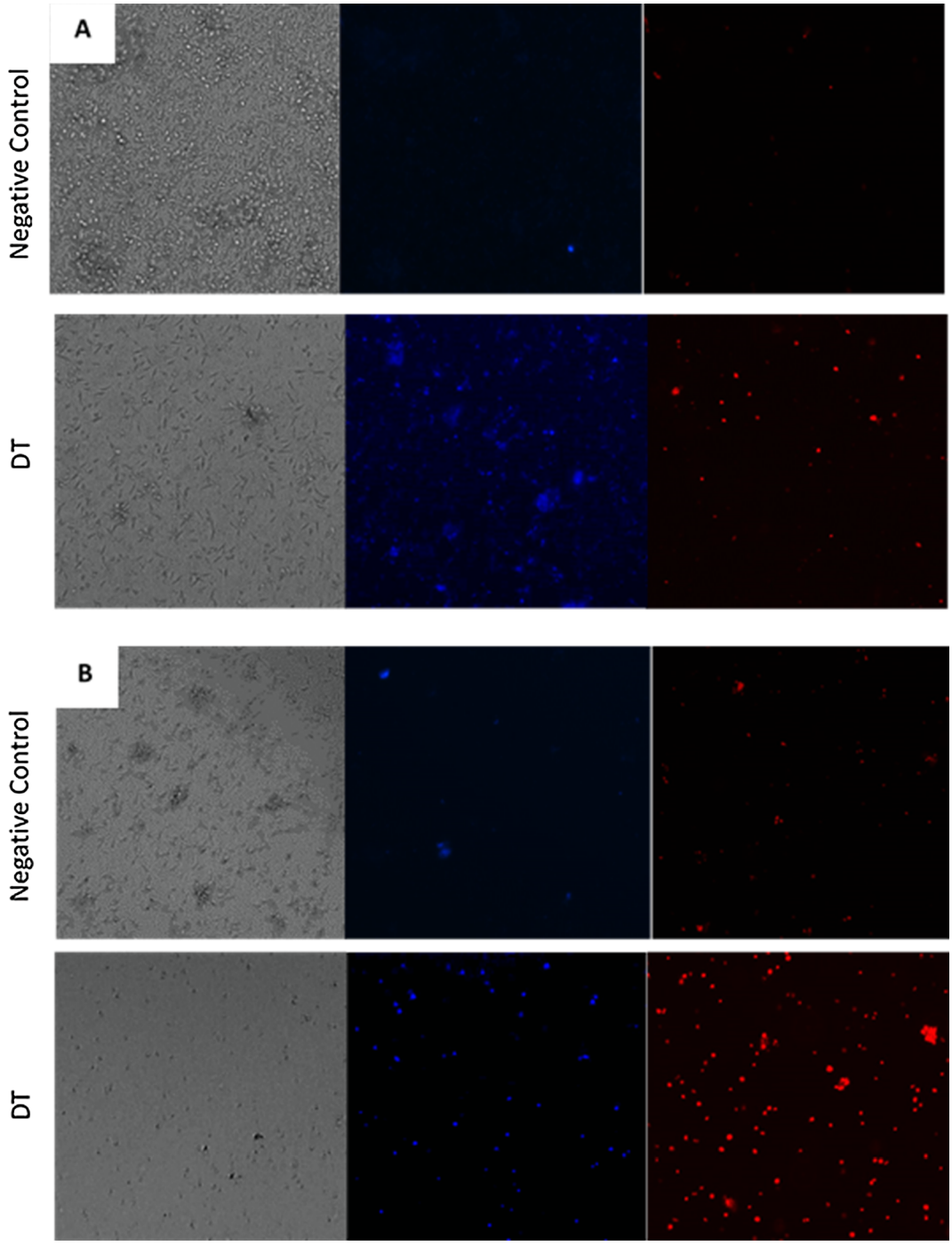

Fig. 2. *Leishmania amazonensis* (A) and *Trypanosoma cruzi* (B) incubated with IC_{90} of DT (**1**) and the evolution of chromatin condensation observed after 24 h. Hoechst stain is different in control cells, where uniformly faint-blue nuclei are observed, and in treated cells, where the nuclei are bright blue. Red fluorescence corresponds to the propidium iodide stain. Images (20X) are showing chromatin condensation (blue) in treated cells. Images (20X) are representative of the cell population observed in the performed experiments. Images were obtained using an EVOS FL Cell Imaging System AMF4300, Life Technologies, USA.

described. These family include the Ser-Thr Protein phosphatase type 2A (PP2A) and integrin inhibitory substances [4–8].

In this study, sixteen oxasqualenoids (Fig. 1), either isolated from the natural source, the red alga *Laurencia viridis*, or obtained by semi-synthetic procedures from the lead compound dehydrothyrsiferol (DT) (**1**), were evaluated in search for trypanocidal or leishmanicidal activity, in order to find new active principles to replace current treatments or to be used as model for their development of new drugs for these diseases.

2. Results and discussion

2.1. Source of the oxasqualenoid compound collection

The samples of oxasqualenoids: dehydrothyrsiferol (DT) (**1**) [9]; thyrsiferol (**2**) [10]; iubol (**3**) [11]; 22-hydroxydehydrothyrsiferol (**4**) [11], 1,2-dehydropseudodehydrothyrsiferol (**5**) [11]; saiyacenols A and B (**6** and **7**) [12]; 28-hydroxysaiyacenol A y B (**8** and **9**) [13], nivariol A (**10**) [14], and the truncated metabolite adejene B (**11**) [15] were obtained in our research group from different collections of the marine red

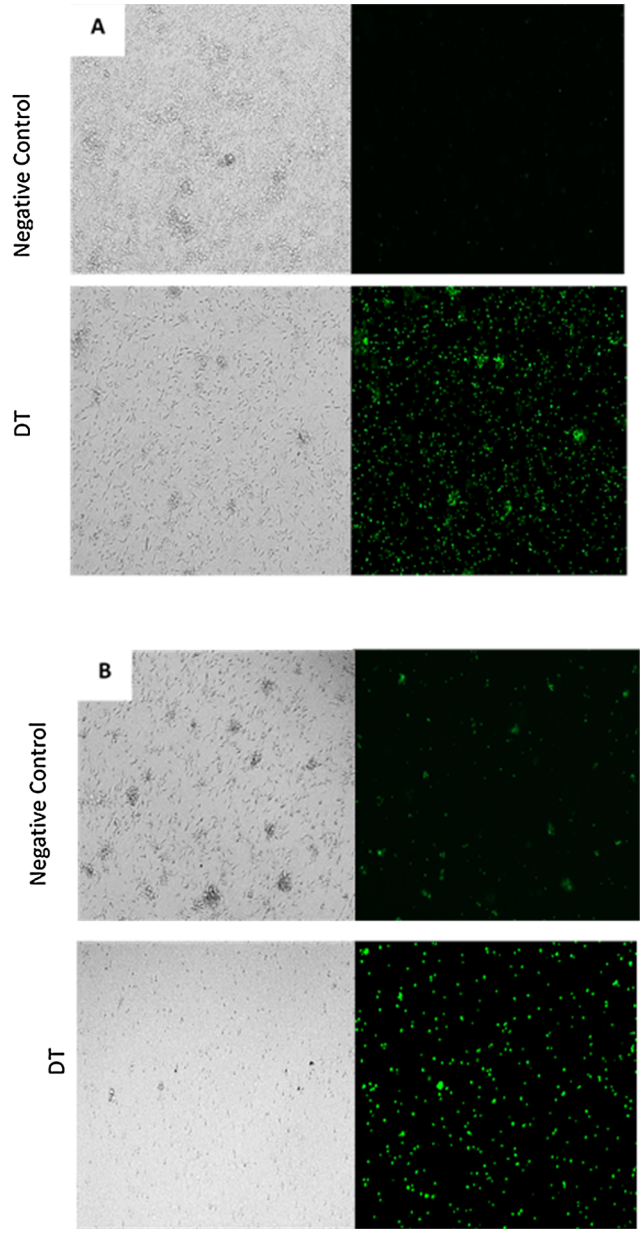

Fig. 3. *Leishmania amazonensis* (A) and *Trypanosoma cruzi* (B) incubated with IC_{90} of DT (**1**) and the evolution of chromatin condensation observed after 24 h. Permeation of the cell plasma membrane to dye SYTOX® green caused by addition of DT (**1**) at IC_{90} for 24 h. DT (**1**) was added to cells (10^6 cells/mL) in the presence of 1 μM SYTOX® green in PBS. Images (40X) are representative of the cell population observed in the performed experiments. Images were obtained using an EVOS FL Cell Imaging System AMF4300, Life Technologies, USA.

algae *Laurencia viridis* during the period 2014–2018. Only DT (**1**) and thyrsiferol (**2**) had been previously obtained from different *Laurencia* species, *L. pinnatifida* [9] and *L. thyrsifera* [10], respectively. In addition, the semi-synthetic congeners: 18-sulphatedehydrothyrsiferol (**12**); 18-ketodehydrothyrsiferol (**13**); 28-iodosaiyacenols A and B (**14** and **15**) and 28-hydroxythyrsiferol (**16**) were prepared from the main metabolite DT (**1**) [16] based on solubility-driven criteria.

2.2. Antiparasitic effects

2.2.1. Antikinetoplastid activities

Initially, eleven natural compounds isolated from specimens of *L. viridis* and five semi-synthetic compounds prepared from DT (**1**) were evaluated for their anti-protozoal activity against three different cell types namely *Leishmania amazonensis* (cutaneous and mucocutaneous leishmaniasis), *Leishmania donovani* (visceral leishmaniasis) and *Trypanosoma cruzi* (Chagas disease). The antikinetoplastid results are summarized in Table 1. Among the tested molecules, six were effective against *L. amazonensis* with an IC_{50} ranged from 5.40 ± 0.13 μM for 28-iodosaiyacenol B (**15**) to 20.39 ± 2.90 μM for 28-iodosaiyacenol A (**14**). *Leishmania donovani* was inhibited by four compounds with IC_{50} values ranged from 18.08 ± 2.62 to 33.90 ± 1.74 μM for iubol (**3**) and 28-iodosaiyacenol A (**14**), respectively. Meanwhile, *Trypanosoma cruzi* was the most resistant parasite with only four effective compounds, namely, iubol (**3**) with an IC_{50} of 9.20 ± 1.16 μM; DT (**1**) with an IC_{50} of 9.45 ± 0.46 μM, 18-ketodehydrothyrsiferol (**13**) with an IC_{50} of 11.02 ± 2.60 μM, and saiyacenol-A (**6**) with an IC_{50} of 13.75 ± 2.28 μM.

Regarding the reference drugs to treat leishmaniasis and Chagas disease, we have evaluated miltefosine and benznidazole, respectively, in order to compare with our compounds. Miltefosine showed an IC_{50} of 6.48 ± 0.24 μM against *L. amazonensis* and 3.32 ± 0.27 μM against *L. donovani* with a CC_{50} of 72.19 ± 3.06 μM, and benznidazole an IC_{50} of 6.94 ± 1.94 μM with a CC_{50} of 400 ± 4 μM [17].

2.2.2. Mechanisms of cell death

DT (**1**) was selected as candidate molecule to analyze its mode of action, based on the antiparasitic results observed and the fact that **1** is the major metabolite in the red alga. *L. amazonensis* and *T. cruzi* were incubated with the IC_{90} of DT (**1**), 29.06 μM and 63.94 μM, respectively. The IC_{90} value was used to increase the population of affected parasites and to reduce the experimental time. As observed in Fig. 2, after 24 h of incubation, treated cells show a higher number of cells with strong blue staining in the nucleus for both *L. amazonensis* and *T. cruzi*. The staining in the nucleus corresponds with the process of chromatin condensation, a very common event on cells suffering an apoptosis-like cell death. Thus, DT (**1**) caused chromatin condensation in treated cells.

DT (**1**) caused plasma membrane permeability in treated cells. As observed in Fig. 3, after 24 h of incubation of the parasite (*Leishmania* and *Trypanosoma*) with the appropriate IC_{90} of DT (**1**), the treated cells show a higher green fluorescence that confirms the plasmatic membrane damage. Even thought, the cell integrity is still maintained.

DT (**1**) induced mitochondrial damage. The effect of the tested compound on the mitochondria membrane potential was confirmed by confocal microscopy (Fig. 4). Moreover, the tested drug could induce the depolarization of (ΔΨm) since the JC-1 dye remained in the cytoplasm in its monomeric form, shown as green fluorescence. The mitochondrial damage has been verified as well by quantifying the ATP level generated in 24 h. We found out that the IC_{90} produced a noticeable decrease in the total ATP level for both parasites (Fig. 5). Furthermore, this effect was dramatically higher in *T. cruzi* with a level of produced ATP lower than 1% of ATP level produced in untreated cells.

There are many differences between the observed effects over both parasites that suggest an advanced death process for *T. cruzi* in comparison with an early stage of death for *L. amazonensis* after 24 h of treatment with DT (**1**). This is confirmed by the higher percentage of parasites stained with propidium iodide in the chromatin condensation assay, the lower level of ATP, and a higher percentage of parasites stained in green (low mitochondrial potential) in the JC-1 assay. In addition, this could be observed on the light transmitted images of the parasites, where the *T. cruzi* parasites look more rounded, smaller and damaged than the *L. amazonensis* ones.

2.2.3. Analysis by Atomic Force microscopy (AFM) of DT effects

In order to establish the structural damage produced by DT (**1**), a detailed study using AFM was carried out on *T. cruzi* (Fig. 6). For this purpose, a negative control of non-treated epimastigotes (10^5 cell/mL) were fixed in smears on a glass surface and the different parts of the

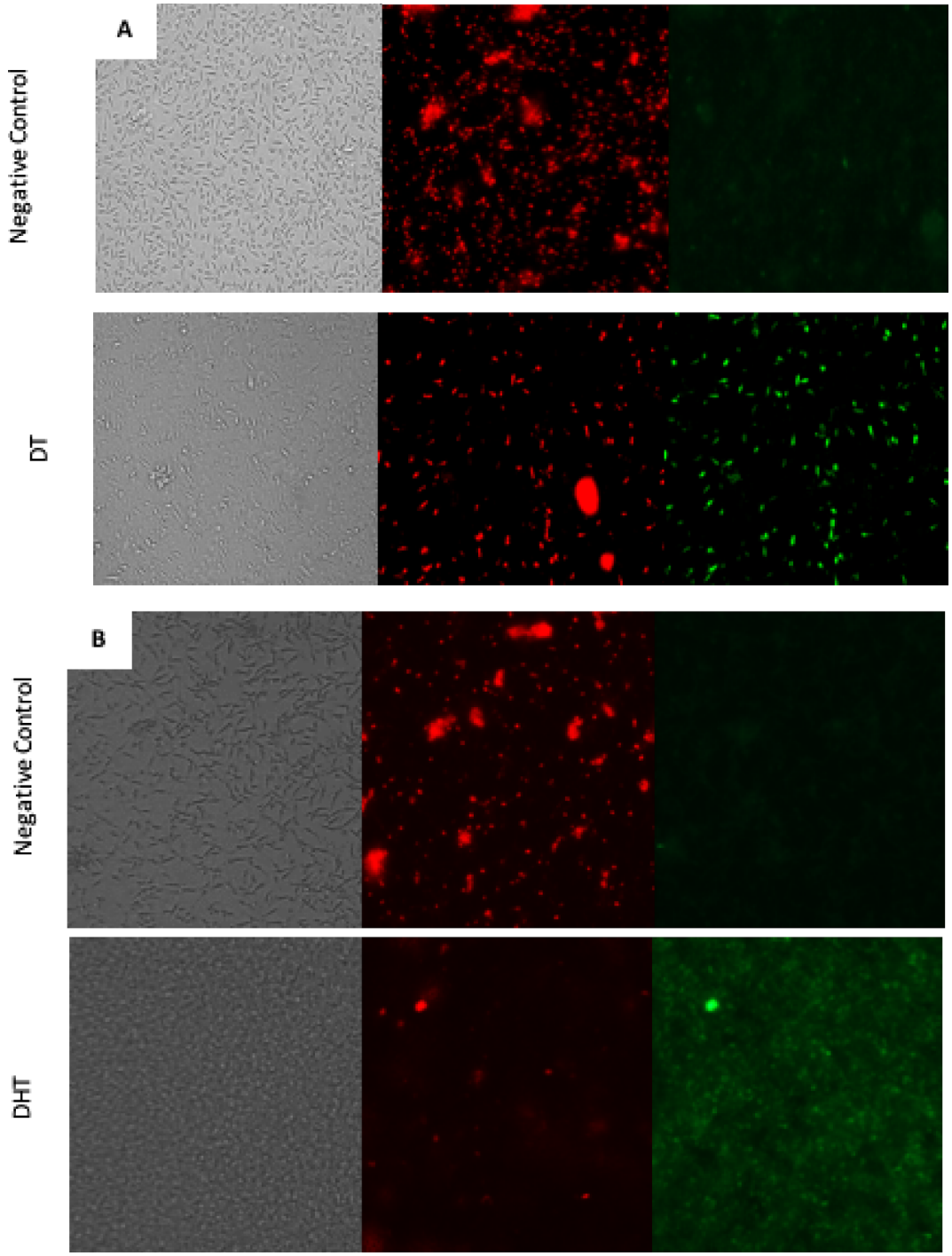

Fig. 4. The effect of DT (**1**) on the mitochondrial membrane potential, in healthy cells, the JC-1 dye accumulates in the mitochondria as aggregates and emit a red fluorescence, meanwhile, in treated cells the dye remained as monomers in the cytoplasm and emit a green fluorescence. (A): *Leishmania amazonensis*; (B): *Trypanosoma cruzi*. Images (40X) are representative of the cell population observed in the performed experiments. Images were obtained using an EVOS FL Cell Imaging System AMF4300, Life Technologies, USA.

parasite were analyzed using AFM. Control images clearly show an intact cell morphology, the flagellar pocket and a normal cell membrane. In the same way, epimastigotes treated with DT (**1**) at IC_{90} for 24 h were equally processed and observed using AFM. The most representative images of the DT (**1**) effects on *T. cruzi* are summarized in Fig. 7. Among the observed effects using this approach, it is important to highlight that key cellular events were observed in treated cells when compared to a non-treated control parasite, such as the loss of intracellular content including the kinetoplast. Moreover, the flagellar pocket was collapsed and the cellular membrane showed dramatic signs of blebbing as it can be observed in Fig. 7.

2.3. Structure-activity relationship analysis

Among the metabolites tested against *Leishmania* and *Trypanosoma*, eight showed activity against parasites (Table 1). A summary of the results from the structural point of view is represented in Fig. 8. Also, the selective index of the most active compounds is shown in Table 2. The structure–activity relationship (SAR) discussion starts using the major compound in the alga, dehydrothyrsiferol (DT) (**1**), as model

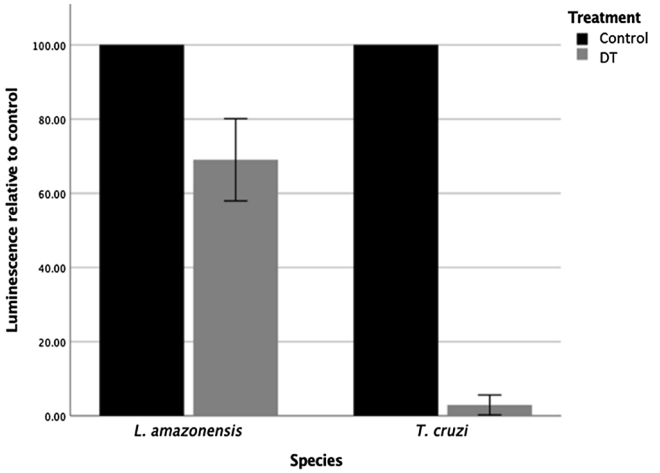

Fig. 5. The effect of DT (**1**) on the ATP level of the parasites after 24 h of treatment. Data are expressed as percentage relative to control. ATP level was measured using a Cell Titer-Glo® Luminescent Cell Viability Assay (Promega).

molecule due to its antiparasitic activity against the three-tested parasite models *L. amazonensis*; *L. donovani* and *T. cruzi* with IC_{50} of 8.36 ± 0.77, 28.26 ± 1.74 and 9.45 ± 0.46 μM, respectively. Thus, the molecular fragments that imply active substances are embedded in different colors associated to the parasite species: *L. amazonensis* are in green squares; *L. donovani* in blue color and the molecules active against *T. cruzi* are marked in red. Simplifications in the size of the molecule as is the case of adejene B (**11**) (fragment C-1-C-14), and bromine losses as for 1,2-dehydropseudodehydrothyrsiferol (**5**) or nivariol A (**10**) lead to inactive substances. In the same way, chemical modifications carried out on DT (**1**): sulfonation at C-18 (e.g. 18-sulphatedehydrothyrsiferol (**12**)), as well as the diol formation at C-15-C-28 (e.g. 28-hydroxythyrsiferol (**16**)), led us to substances with no activity. On the other hand, the modification of the tetrahydrofuran terminal ring between C-19 and C-22 by a tetrahydropyran ring between C-19 and C-23 leads us to the most active and toxic compound against murine macrophage J774A.1, iubol (**3**). The sole oxidation of DT (**1**) at C-22 in 22-hydroxydehydrothyrsiferol (**4**) lead us to a less active substance against *L. amazonensis* than (**1**), with an IC_{50} of 34.65 ± 0.22 μM and inactive against *L. donovani* and *T. cruzi*. In the case of the additional introduction of a hydroxyl group at carbon C-15 (e.g. thysiferol (**2**)), it produces a total loss of activity. Moreover, oxidation at C-18 (e.g. 18-ketodehydrothyrsiferol (**13**)) lead to a compound with antiparasitic properties against *L. amazonensis*; *L. donovani* and *T. cruzi,* but showing less effectivity than the model molecule.

The most interesting series of analogues from the SAR point of view is represented by the pentacyclic compounds **6**–**9**, **14** and **15**, with an additional tetrahydrofuran ring between C-15 and C-18. Thus, the intramolecular cyclization produced by attack of the oxygen at C-18 on C-15 leads to a mixture of epimers, saiyacenol A (**6**) and saiyacenol B (**7**). Compound **6** turned out to be active against *L. amazonensis* and *T. cruzi* with an IC_{50} of 12.96 ± 1.84 and 13.75 ± 2.28 μM, respectively. However, its *15R*-isomer, compound **7**, turned out to be slightly more active and selective against *L. amazonensis*, IC_{50} 10.32 ± 1.09 μM, and inactive against *L. donovani* and *T. cruzi*. Oxidation at C-28 (e.g. 28-hydroxysaiyacenols A (**8**) and B (**9**)) produces a similar effect than in thyrsiferol (**2**) case, leading to molecules which lack antikinetoplastid activity. Finally, the introduction of a iodine atom at C-28 in this series leads to selective compounds against *Leishmania* species, 28-iodosaiyacenols A (**14**) and B (**15**). This modification turned out to be the most effective transformation obtaining a new lead, 28-iodosaiyacenol B (**15**), with notable activity against *L. amazonesis* (IC_{50} 5.40 ± 0.13 μM) that turned out to be non-toxic against the murine macrophage cell line J774A.1 (CC_{50} > 100). Its activity is comparable to that of the reference drug miltefosine (IC_{50} 6.48 ± 0.24 and CC_{50} 72.19 ± 3.06 μM (Table 1; Fig. 8).

In addition, the activity of DT (**1**) against the amastigote stage of *L. amazonensis* is better than miltefosine, showing an IC_{50} of 2.16 ± 0.20 μM for DT (**1**) compared with the IC_{50} 3.12 ± 0.30 μM of miltefosine. This stage of the parasite corresponds with that present in the host, being the infective form and causative of the pathology. However, the cytotoxicity of the compound does not allow DT (**1**) to improve the selectivity index of miltefosine. For *T. cruzi*, neither compound showed better activity than benznidazole, nor selectivity index, due to the low cytotoxic effect of benznidazole. Consequently, the results hereby presented confirm that secondary metabolites of the red alga *L. viridis* show great biological properties and adequate antiparasitic drugs may become available from them.

3. Experimental section

3.1. General methods

All reagents were commercially available and used as received. All solvents were dried and distilled under argon immediately prior to use or stored appropriately. Flash chromatography was performed with silica gel (230–400 mesh) as the stationary phase and mixtures of *n*-hexane and EtOAc, in different proportions given in each case, as the mobile phase. EnSpire® Multimode Reader (Perkin Elmer, Waltham, MA, USA) using absorbance values of Alamar Blue® reagent (Bio-Rad Laboratories, Oxford, UK). TLC was performed on AL Si gel. TLC plates were visualized by UV light (254 nm) and by adding a phosphomolybdic acid solution 10 wt% in MeOH or a vanillin solution (6 g of vanillin, 450 mL of EtOH, 40 mL of AcOH, and 30 mL of H_2SO_4).

3.2. Isolation of Laurencia metabolites and chemical transformations

Natural metabolites were isolated from the seasonal red alga *Laurencia viridis* by annual harvestings between April 2013 – April 2018 at Paraiso Floral, Tenerife, Canary Islands (28°07′12″ N, 16°46′45″ W). Dried material of different parts of alga was filed at TFC Phyc 7180 (Herbario de la Universidad de La Laguna, Departamento de Biología Vegetal, Botánica, Tenerife, Spain).

Standard procedure for the isolation of marine polyether triterpenoids starting by extraction of dry alga *L. viridis* with $CHCl_3$:MeOH (1:1) at room temperature (rt), and a dark green, viscous oil were obtained after concentration under reduced pressure. The extracts were first chromatographed on Sephadex LH-20 (7 × 50 cm) using CH_2Cl_2:MeOH (1:1) as the mobile phase. The oxasqualenoid fractions were subsequently processed on a silica gel column with *n*-hexane:EtOAc (4:1–1:4) and medium-pressure chromatography was done on Lobar LiChroprep Si-60 using CH_2Cl_2:acetone (4:1) at 1 mL/min. Final purification was done on a HPLC with a μ-Porasil column using *n*-hexane:EtOAc:MeOH, 18:15:5 to yielded pure compounds: dehydrothyrsiferol (DT) (**1**); thyrsiferol (**2**); iubol (**3**); 22-hydroxydehydrothyrsiferol (**4**); 1,2-dehydropseudodehydrothyrsiferol (**5**); saiyacenols A and B (**6** and **7**); 28-hydroxysaiyacenols A and B (**8** and **9**); nivariol A (**10**) and the truncated metabolite adejene B (**11**) were obtained for the biological assays. 18-sulphatedehydrothyrsiferol (**12**); 18-ketodehydrothyrsiferol (**13**); 28-iodosaiyacenols A and B (**14** and **15**) and 28-hydroxythyrsiferol (**16**) were prepared from the main metabolite DT (**1**) using the methodology previously described [16], and purified by HPLC with a μ-Porasil column using *n*-hexane:EtOAc:MeOH, 18:15:5.

3.3. Parasite strain

The activity of different compounds was evaluated against promastigotes and amastigote stage of *L. amazonensis* (MHOM/BR/77/LTB0016) and epimastigote *T. cruzi* (Y strain). Cytotoxicity assays of the active molecules was tested against the macrophage J774A.1 cell line,

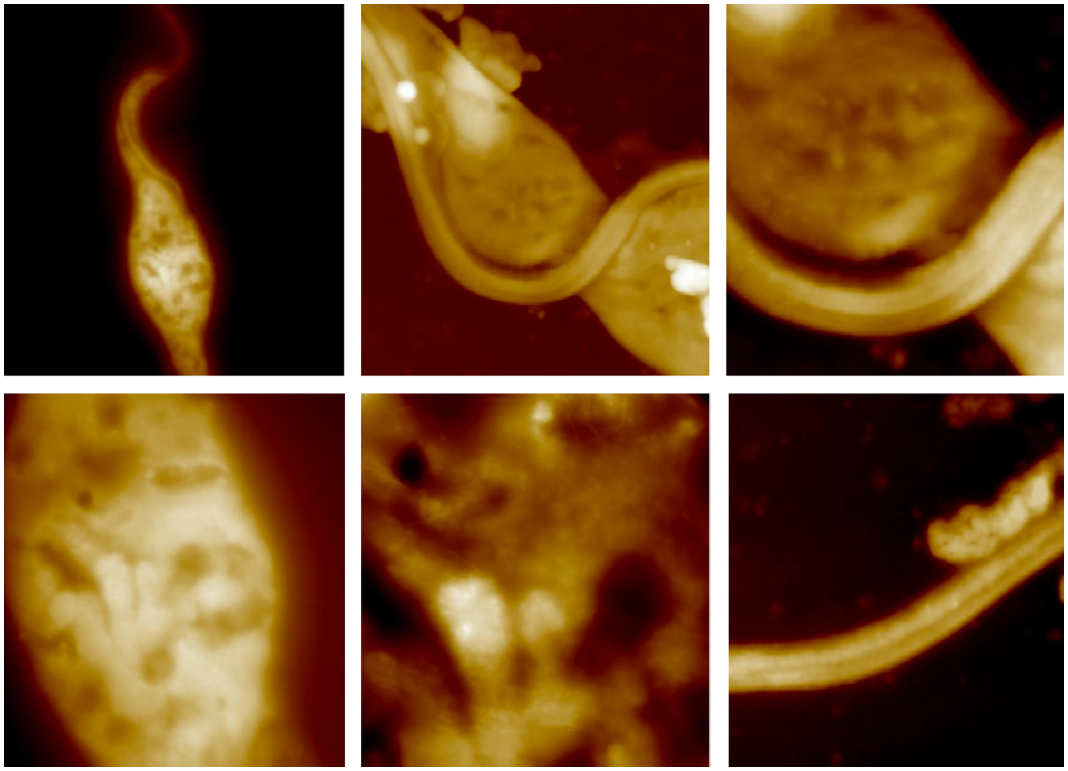

Fig. 6. AFM image of epimastigotes of *Trypanosoma cruzi.* Details of the parasite and the flagella. Images size: top, left-right 20 × 20; 4 × 4; 2 × 2 μmxμm; bottom, left-right 6.1 × 6.1; 3 × 3; 2.7 × 2.7 μm × μm).

cultured in RPMI 1640 medium supplemented with 10% fetal bovine serum at 37 °C and 5% CO_2 atmosphere. Promastigotes of both strains of *Leishmania* were cultured in Schneider's medium (Sigma-Aldrich, Madrid, Spain) supplemented with 10% fetal bovine serum at 26 °C and were grown to the log phase per previous methods for use in further experiments. For some of the assays, the parasites were also cultured in RPMI 1640 medium (Gibco), with or without phenol red. Epimastigotes of both strains were cultured in Liver Infusion Tryptose (LIT) medium supplemented with 10% fetal bovine serum at 26 °C and were grown to the log phase for use in further experiments.

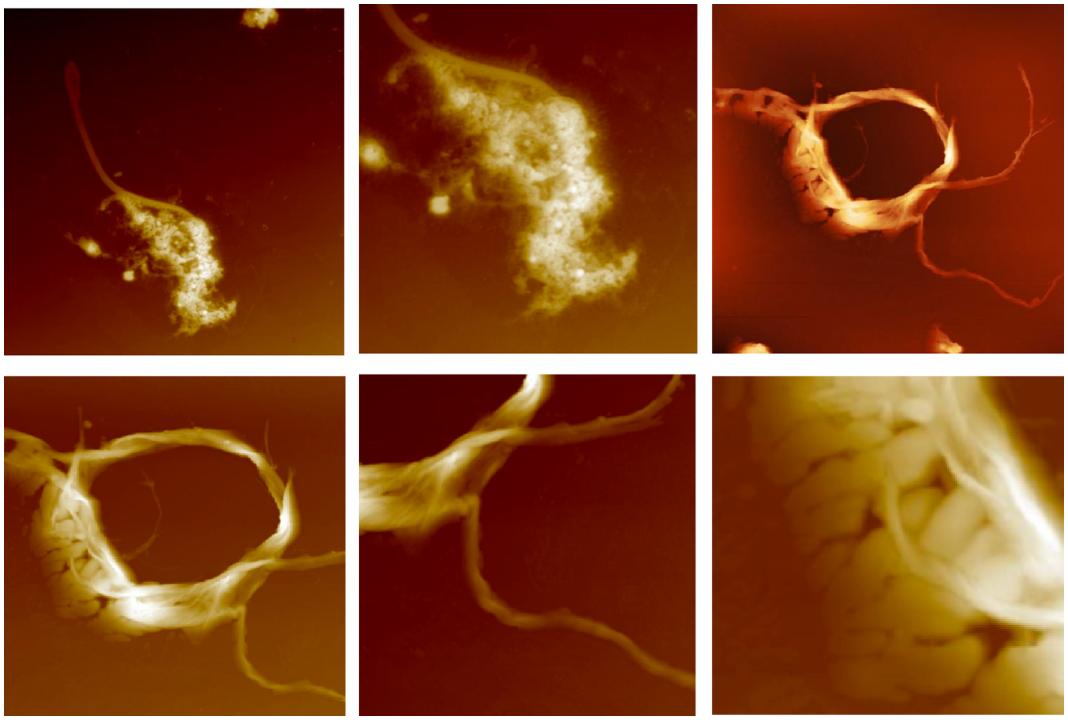

Fig. 7. AFM image of epimastigotes of *Trypanosoma cruzi* treated with DT (**1**) IC_{90} during 24 h. Details of the parasite and the flagella. Images size: top, left-right 20x20; 10.9 × 10.9; 31.3 × 31.3 μm × μm; bottom, left-right 20 × 20; 15 × 15; 7.5 × 7.5 μm × μm).

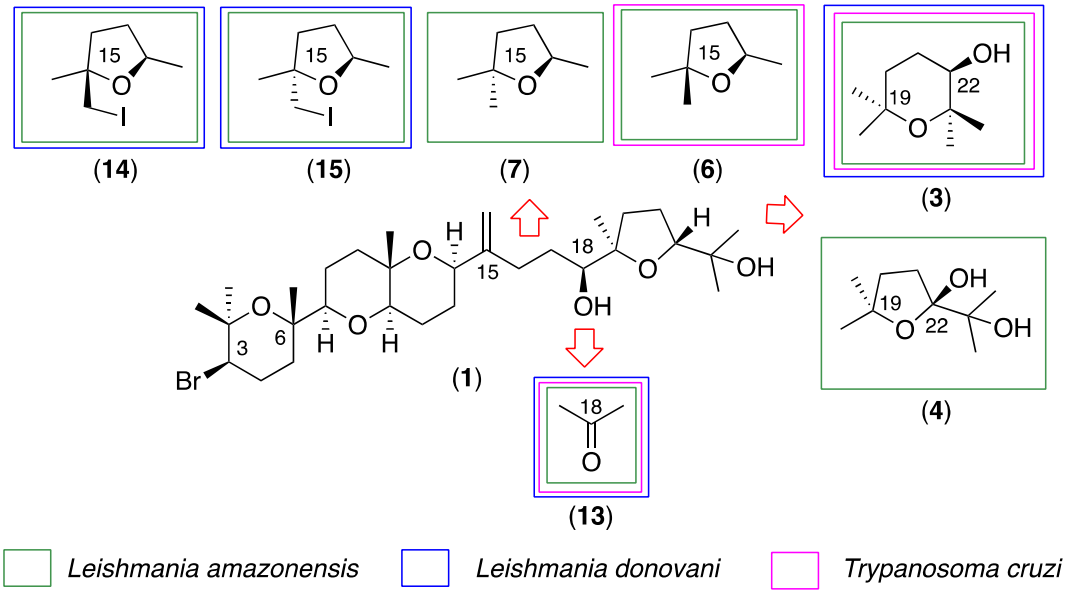

Fig. 8. Structure activity relationship (SAR) for oxasqualenoids with antikinetoplastid properties based on the main metabolite DT (**1**) as lead molecule. Color squares correlate the active substances *vs* species.

3.4. Evaluation of leishmanicidal, trypanocidal and cytotoxic activities

3.4.1. Leishmanicidal capacity assay

Logarithmic phase cultures of promastigote stage of *L. amazonensis* were used for experimental purposes, and the in vitro susceptibility assay was performed in sterilized 96-well plates. 10^6/well parasites were added to wells containing different concentration of the drug to be tested. Percentages of inhibition, 50% inhibitory concentrations (IC_{50}) for active compounds were calculated by linear regression analysis using the alamarBlue® method [18]. Subsequently, the most active molecules were tested against the intra-macrophages stage of *L. amazonensis*.

The anti-amastigote activity was measured according to Jain *et al.* [20]. Macrophages of the J774A.1 cell line were placed in a 96-well flat bottom plate at a density of 2×10^5/mL in RPMI-1640 supplemented with 10% SBF and was incubated for an hour at 37 °C in a 5% CO_2 environment to allow almost complete differentiation of the cells. 100 µL of stationary phase promastigotes (7 days old culture) were added in a 10:1 ratio and the cultures (2×10^6/mL) and were re-incubated at 37 °C for 24 h to allow a maximum infection. After the incubation, the excess of promastigotes was washed off with the same medium at least 3 times. 50 µL of the culture medium (RPMI-1640 with 10% FBS) were added into each well. In the same time, a serially dilution of the test compounds was made in a 96-deep well plate with the same medium, and then 50 µL of this serially-diluted standard were added to each well. The plates were incubated at 37 °C, 5% CO_2 for 24 h. After this incubation, we remove the medium from each well and add 30 µL of Schneider (with 0.05% SDS) was added to each well. The plate was shacked for 30 s and 170 µL of Schneider medium were added to each well. alamarBlue at 10% was added into each well of the 96-well plates and incubated at 26 °C for 72 h to allow the transformation of rescued amastigote to promastigotes. After overnight incubation, the plates were read in a spectrofluorimeter at 544 nm excitation, 590 nm emission.

Table 2
Selectivity Index (SI = CC_{50}/IC_{50}) of active oxasqualenoids and reference drugs against *L. amazonensis, L. donovani* and *T. cruzi* referred to toxicity against murine macrophage J774.A1.

Compounds	*L. amazonensis* (Promastigote)	*L. donovani* (Promastigote)	*T. cruzi* (Epimastigote)
1	3.4	1.0	3.0
3	1.1	0.4	0.8
4	2.9	NA	NA
6	4.6	NA	4.4
7	> 9.7	NA	NA
13	0.6	0.5	2.1
14	1.4	0.9	NA
15	> 18.5	> 5.9	NA
Miltefosine*	11.1	21.7	–
Benznidazole*	–	–	57.6

NA: Not active at the maximum concentration tested.
* Reference compounds.

3.4.2. Trypanocidal capacity assay

The activity was evaluated *in vitro* against epimastigote stage of *T. cruzi*. Different concentrations of fractions and compounds were incubated in 96 wells plate for 96 h with a density of 10^5 parasite/well. 10% of alamarBlue® was added to each well and the IC_{50} was calculated. All assays have been realized in triplicate.

3.4.3. Cytotoxicity assay

The cytotoxicity of active compounds was evaluated in J774A.1 macrophages cell line. Serial dilution of compounds **1–16** were plated and incubated with the appropriate cell concentration of macrophages. After 24 h cell viability was determined using alamarBlue® method using dose response curves to obtain the CC_{50} [19].

3.5. Mechanisms of cell death

3.5.1. Chromatin condensation determination

A double-stain apoptosis detection kit (Hoechst 33342/PI) (GenScript, Piscataway, NJ, USA) and an EVOS FL Cell Imaging System AMF4300, Life Technologies, USA were used. The experiment was carried out by following the manufacturer's recommendations, briefly, after being treated with IC_{90} of the tested molecules for 24 h, cells were centrifuged (1500 rpm for 10 min) washed twice with PBS (phosphate buffered saline) buffer. The double-staining pattern allows the identification of three groups in a cellular population: live cells will show only a low level of fluorescence, cells undergoing PCD will show a higher level of blue fluorescence (as chromatin condenses), and dead cells will show low-blue and high-red fluorescence (as the propidium iodide stain enters the nucleus).

3.5.2. Plasma membrane permeability

The SYTOX® Green assay was performed to detect membrane permeability alterations of parasites. Briefly, 1×10^7 parasites/mL were washed and incubated in PBS with the of SYTOX® Green at a final concentration of 1 μM (Molecular Probes) for 15 min in the dark at room temperature. Subsequently the tested compounds were added at IC_{90} concentration. The increase in fluorescence due to binding of the fluorescent marker to the parasitic DNA was observed in an EVOS FL Cell Imaging System AMF4300, Life Technologies, USA.

3.5.3. Analysis of mitochondrial membrane potential

The collapse of an electrochemical gradient across the mitochondrial membrane during apoptosis was measured using a JC-1 Mitochondrial Membrane, Potential Assay Kit, Cayman Chemical. After being treated with IC_{90} concentration of the tested molecules for 24 h, the promastigotes were centrifuged (1500 rpm × 10 min) and suspended in JC-1 buffer. After that, 100 μL of each treated culture was added to a black 96 well plate (PerkinElmer) than 10 μL of JC-1 was added and incubated at 26 °C for 30 min. Analysis for mean green and red fluorescence intensity was done using an Enspire microplate reader (PerkinElmer, Massachusetts, USA) for 30 min. In addition, the depolarization of the mitochondrial membrane potential was confirmed by microscopic observation using EVOS FL Cell Imaging System AMF4300, Life Technologies, USA.

3.5.4. Measurement of ATP

ATP level was measured using a Cell Titer-Glo® Luminescent Cell Viability Assay (Promega). The effect of the drug on the ATP production was evaluated by incubating (10^7 cells/mL) with the previously calculated IC_{90} of the tested molecules.

3.6. Atomic Force microscopy (AFM) analysis

A culture of *T. cruzi* was incubated with DT (**1**) at final concentration IC_{90} for 24 h. After the incubation, 10 μL of the culture contained 10^5 cell/mL was smeared on glass slides. Samples were dried during 10 min before AFM analysis. AFM topographic images were obtained in Peak Force mode using a multimode microscope with a Nanoscope V control unit from Bruker. Scan rates of 0.5–1.2 Hz and FESP (50–100 kHz, and 1–5 $N\,m^{-1}$) tips (from Bruker) were used. To get representative information about the damage process in *T. cruzi* caused by DT (**1**), images from (100 μm × 100 μm) to (0.6 μm × 0.6 μm) were recorded using 512 points/line.

3.7. Statistical analysis

The Percentage of inhibition and 50% inhibitory concentration (IC_{50}) and the cytotoxicity concentration were determined by non-linear regression analysis with 95% confidence limits. All experiments were performed three times each in duplicate and the mean values were also calculated. A Turkey test was used for analysis of the data. Values of $p < 0.05$ were considered significant. The one-way ANOVA statistical analysis was undertaken using the SPSS Statistics 25.

Acknowledgements

This work was funded by INTERREG-MAC/1.1b/042 (BIOTRANSFER2), PI18/01380 from Instituto de Salud Carlos III, Spain and RICET [RD16/0027/0001 project, from Programa Redes Temáticas de Investigación Cooperativa, FIS (Ministerio Español de Salud, Madrid, Spain), FEDER. IS, ALA and ARDM were funded by the Agustín de Betancourt Programme (Cabildo de Tenerife – ULL). Authors acknowledge the use AFM Service of General Research Support Services of University of La Laguna (SEGAI-ULL).

References

[1] WHO|World Health Organization. Neglected tropical diseases. 2019. < http://www.who.int/neglected_diseases/diseases/en/. Accessed Apr 19, 2019 > .
[2] S.P.S. Rao, M.P. Barrett, G. Dranoff, C.J. Faraday, C.R. Gimpelewicz, A. Hailu, C.L. Jones, J.M. Kelly, J.K. Lazdins-Helds, P. Mäser, J. Mengel, J.C. Mottram, C.E. Mowbray, D.L. Sacks, P. Scott, G.F. Späth, R.L. Tarleton, J.M. Spector, T.T. Diagana, Drug discovery for kinetoplastid diseases: Future directions, ACS Infect. Dis. 5 (2019) 152–157.
[3] P.L. Bustos, N. Milduberger, B.J. Volta, A.E. Perrone, S.A. Laucella, J. Bua, *Trypanosoma cruzi* infection at the maternal-fetal interface: Implications of parasite load in the congenital transmission and challenges in the diagnosis of infected newborns, Front. Microbiol. 10 (2019) 1250, https://doi.org/10.3389/fmicb.2019.01250.
[4] J.J. Fernández, M.L. Souto, M. Norte, Marine polyether triterpenes, Nat. Prod. Rep. 17 (2000) 235–246.
[5] M.L. Souto, C.P. Manríquez, M. Norte, F. Leira, J.J. Fernández, The inhibitory effects of squalene-derived triterpenes on protein phosphatase PP2A, Bioorg. Med. Chem. Lett. 13 (2003) 1261–1264.
[6] M.K. Pec, A. Aguirre, K. Moser-Thier, J.J. Fernández, M.L. Souto, J. Dorta, F. Díaz-González, J. Villar, Induction of apoptosis in estrogen dependent and independent breast cancer cells by the marine terpenoid dehydrothyrsiferol, Biochem. Pharmacol. 65 (2003) 1451–1461.
[7] M.K. Pec, M. Artwohl, J.J. Fernández, M.L. Souto, D. Álvarez de la Rosa, T. Giraldez, A. Valenzuela-Fernández, F. Díaz-González, Chemical modulation of VLA integrin affinity in human breast cancer cells, Exp. Cell Res. 313 (2007) 1121–1134.
[8] F. Cen-Pacheco, J.A. Villa-Pulgarin, F. Mollinedo, M. Norte, A.H. Daranas, J.J. Fernández, Cytotoxic oxasqualenoids from the red alga *Laurencia viridis*, Eur. J. Med. Chem. 46 (2011) 3302–3308.
[9] A.G. González, J.M. Arteaga, J.J. Fernandez, J.D. Martin, M. Norte, J.Z. Ruano, Terpenoids of the red alga *Laurencia pinnatifida*, Tetrahedron 40 (1984) 2751–2755.
[10] J.W. Blunt, M.P. Hartshorn, T.J. McLennan, M.H.G. Munro, W.T. Robinson, S.C. Yorke, Thyrsiferol: a squalene-derived metabolite of *Laurencia thyrsifera*, Tetrahedron Lett. 19 (1978) 69–72, https://doi.org/10.1016/S0040-4039(01)88986-3.
[11] F. Cen-Pacheco, J.A. Villa-Pulgarin, F. Mollinedo, M. Norte Martín, J.J. Fernández, A.H. Daranas, New polyether triterpenoids from *Laurencia viridis* and their biological evaluation, Mar. Drugs 9 (2011) 2220–2235, https://doi.org/10.3390/md9112220.
[12] F. Cen-Pacheco, F. Mollinedo, J.A. Villa-Pulgarin, M. Norte, J.J. Fernández, A.H. Daranas, Saiyacenols A and B: the key to solve the controversy about the configuration of aplysiols, Tetrahedron 68 (2012) 7275–7279, https://doi.org/10.1016/j.tet.2012.07.005.
[13] F. Cen-Pacheco, A.J. Santiago-Benítez, C. García, S.J. Álvarez-Méndez, A.J. Martín-Rodríguez, M. Norte, V.S. Martín, J.A. Gavín, J.J. Fernández, A.H. Daranas, Oxasqualenoids from *Laurencia viridis*: Combined spectroscopic–computational analysis and antifouling potential, J. Nat. Prod. 78 (2015) 712–721, https://doi.org/10.1021/np5008922.
[14] F. Cen-Pacheco, J. Rodríguez, M. Norte, J.J. Fernández, A.H. Daranas, Connecting discrete stereoclusters by using DFT and NMR spectroscopy: the case of nivariol, Chem. Eur. J. 19 (2013) 8525–8532, https://doi.org/10.1002/chem.201204272.
[15] F. Cen-Pacheco, L. Nordström, M.L. Souto, M. Norte Martín, J.J. Fernández, A.H. Daranas, Studies on polyethers produced by red algae, Mar. Drugs 8 (2010) 1178–1188, https://doi.org/10.3390/md8041178.
[16] J. Lorenzo-Morales, A.R. Díaz-Marrero, F. Cen-Pacheco, I. Sifaoui, M. Reyes-Batlle, M.L. Souto, A.H. Daranas, J.E. Piñero, J.J. Fernández, Evaluation of oxasqualenoids from the red alga *Laurencia viridis* against *Acanthamoeba*, Mar. Drugs 17 (2019) 420, https://doi.org/10.3390/md17070420.
[17] A. López-Arencibia, D. García-Velázquez, C.M. Martín-Navarro, I. Sifaoui, M. Reyes-Batlle, J. Lorenzo-Morales, In vitro activities of hexaazatrinaphthylenes against *Leishmania* spp, Antimicrob. Agents Chemother. 59 (2015) 2867, https://doi.org/10.1128/AAC.00226-15.
[18] I. Sifaoui, A. López-Arencibia, C.M. Martín-Navarro, N. Chammem, M. Reyes-Batlle, M. Mejri, J. Lorenzo-Morales, M. Abderabba, J.E. Piñero, Activity of olive leaf extracts against the promastigote stage of Leishmania species and their correlation with the antioxidant activity, Exp. Parasitol. 141 (2014) 106–111.
[19] H. Fadel, I. Sifaoui, A. López-Arencibia, M. Reyes-Batlle, S. Hajaji, O. Chiboub, I.A. Jiménez, I.L. Bazzocchi, J. Lorenzo-Morales, S. Benayache, J.E. Piñero, Assessment of the antiprotozoal activity of *Pulicaria inuloides* extracts, an Algerian medicinal plant: leishmanicidal bioguided fractionation, Parasitol. Res. 117 (2018) 531–553.
[20] S.K. Jain, R. Sahu, L.A. Walker, B.L. Tekwani, A parasite rescue and transformation assay for antileishmanial screening against intracellular *Leishmania donovani* amastigotes in THP1 human acute monocytic leukemia cell line, J. Vis. Exp. 70 (2012) 4054, https://doi.org/10.3791/4054.